Scale Effects in Flume Experiments on Flow around a Spur Dike in Flatbed Channel

Robert Ettema[1] and Marian Muste[2]

Abstract: This paper presents the findings from a series of flume experiments conducted to determine scale effects in small-scale models of flow around a single spur dike (wing-dam, groyne, or abutment) placed in a channel whose bed is fixed and flat. The flow features of primary interest are flow-thalweg alignment (line of maximum streamwise velocity) around a dike, and area extent of the flow-separation region (wake) immediately downstream of the dike. Those features are of practical concern in the deployment of dikes for various channel control purposes. The scale effects of concern herein are those attributable to use small length scales together with a bed-shear stress parameter (e.g., Shields parameter) as the primary criterion for dynamic similitude. Small-scale models, especially micromodels, often are used for investigating channel-control issues. Also, the shear-stress criterion is commonly used for models of flow in loose-bed channels, whereas Froude number commonly is the primary similitude criterion for models of fixed-bed open-channel flows. The experiments show that use of a shear-stress parameter as the primary criterion for dynamic similitude influences the flow thalweg and flow separation region at a dike. It does so by distorting pressure gradients around the model dike and by affecting turbulence generated by the dike. It also is shown that, for a range of small models, thalweg alignment and extent of separation region do not scale with model length scales. These findings are important for interpreting results from small hydraulic models, especially micromodels, of flow in loose-bed channels.

DOI: 10.1061/(ASCE)0733-9429(2004)130:7(635)

CE Database subject headings: Hydraulic models; Open channel flow; Dikes; Rivers; Flumes.

Introduction

The principal contribution of this paper is a delineation of scale effects incurred with the use of small hydraulic models to simulate two features of flow around a single dike in a flatbed channel. The features of interest are flow-thalweg alignment (or alignment of the maximum flow velocity) around a dike, and the area extent of the flow-separation or wake region downstream of a dike. Thalweg alignment and wake region are important in the use of spur dikes for diverse channel-control purposes. Of concern, however, is the veracity of small, loose-bed hydraulic models to simulate those flow features. Because dynamic similitude for loose-bed models commonly is based on a bed-shear-stress (or shear-velocity) criterion associated with a required level of bed-sediment mobility in the model (Hydraulic Modeling 2000), such models may not adequately replicate the local flow field around a dike, and thereby not adequately replicate thalweg position and flow separation around a model dike. Flow inertia and gravity forces, not to mention the effects of viscosity and surface tension, are important in the simulation of flow around a structure.

The writers conducted series of flume experiments using single dikes placed in flatbed flumes with the aim of determining how decreasing length scales, together with the use of a shear-stress (shear velocity) similitude parameter, affect thalweg alignment and the flow separation. The experiments focused especially on the distance required for flow symmetry to recover downstream of a dike in a straight flatbed channel. That information is useful in designing dike length and location. Two measures were used in this respect (Fig. 1): the channel length, T_D, needed for the thalweg to return to the center channel; and the downstream extent of the flow-separation region behind a dike, B_1. Flumes with fixed flat beds were used so as to avoid, for the moment, complication issues attendant to scaling of bedforms and scour.

The experiments were part of a study to determine how accurately very small hydraulic models of flow in open channels, notably micromodels, can simulate flow around spur dikes; Ettema and Muste (2002) document the study. Over the past few years, several districts of the U.S. Army Corps of Engineers (USACE) have used remarkably small hydraulic models (dubbed micromodels by the USACE) to aid in the design of channel-control works. Such models typically reduce the plan area of a multimile river reach to the convenient size of a tabletop, measuring about 2 m long by 1 m wide. Flow depths in the model range from about 10 to 50 mm. The commensurate horizontal scale (herein, scale is defined as prototype/model ratio) of micromodels typically is of the order of about 10^4, and vertical scale is about 10^3; the exact scales vary with the dimensions of channel simulated. The smallness of the micromodels, and commensurately their substantial vertical distortion, raise questions about the capacity of micromodels to simulate alluvial-channel processes, especially the flow fields around hydraulic structures such as channel-control dikes.

Flow around Dikes

Many laboratory studies exist of the flow fields around linear structures such as dikes, abutments, low walls and fences, and

[1]Professor, Dept. of Civil and Environmental Engineering, The Univ. of Iowa, Iowa City, IA 52242.

[2]Research Engineer, IIHR—Hydroscience and Engineering, The Univ. of Iowa, Iowa City, IA 52242.

Note. Discussion open until December 1, 2004. Separate discussions must be submitted for individual papers. To extend the closing date by one month, a written request must be filed with the ASCE Managing Editor. The manuscript for this paper was submitted for review and possible publication on October 29, 2002; approved on October 30, 2003. This paper is part of the ***Journal of Hydraulic Engineering***, Vol. 130, No. 7, July 1, 2004. ©ASCE, ISSN 0733-9429/2004/7-635–646/$18.00.

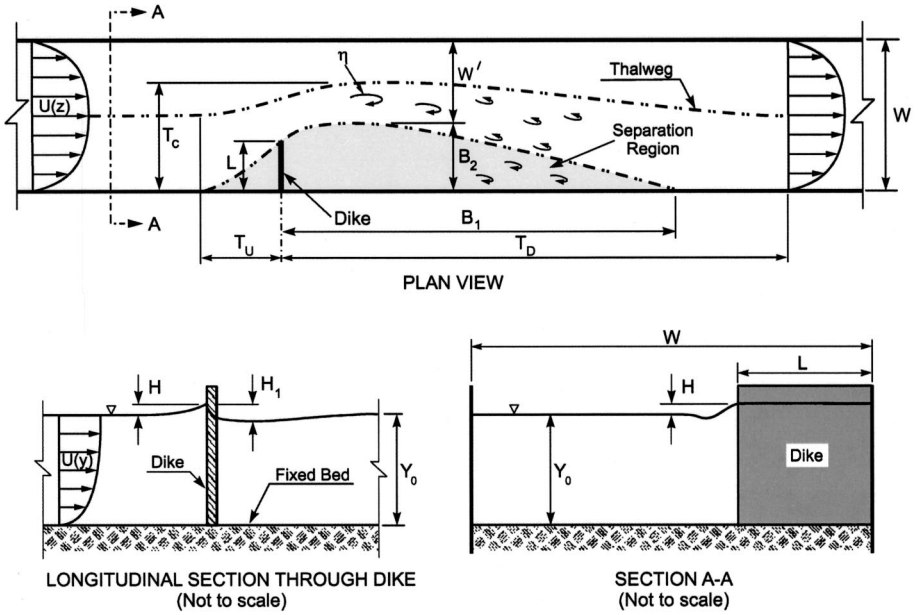

Fig. 1. Flow thalweg and separation around a single dike in a flatbed channel of fixed width

through diverse orifices formed by walls. Additionally, numerous studies exist of scour caused by structures in loose-bed channels. For dikes, however, few studies have investigated the effects of length scale on thalweg alignment and separation regions around a dike; and no study has investigated whether those flow features are affected by dynamic similitude based on bed-particle mobility rather than Froude number. Moreover, there appears to be a lack of detailed mapping of the flow field, or even the thalweg around a full-scale dike. Fairly numerous aerial views exist of flows around dikes, such as Fig. 2, in which drifting ice usefully delineate dike deflection of flow thalweg and dike wake. Full-scale data do exist for portions of flow fields in close proximity to dikes (e.g., Uijttewaal et al. 2001), and on scour and sediment deposition at dikes and abutments (e.g., Brinke et al. 1999).

Reviewed briefly here are prior studies on flow around dikes and abutments. Those studies, however, are not particularly instructive for the purpose of the present study. More useful are several rather early studies on flow around low walls used for developing boundary-layer flow in a wind tunnel, and on flow through orifice plates in pipes. A considerable amount of information exists on the behavior of flow around two-dimensional walls and flow through two-dimensional and symmetric orifices.

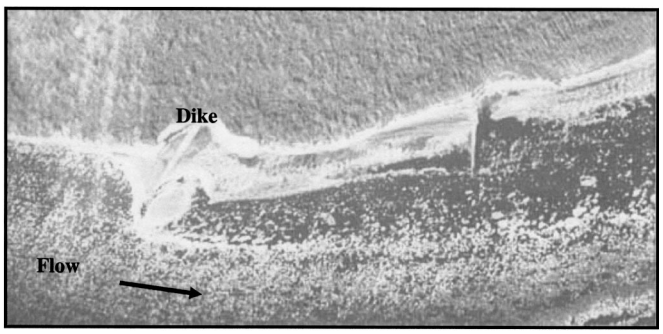

Fig. 2. Drifting ice delineates flow pattern around a dike in the Mississippi River

Flow around Dikes and Abutments

Fairly numerous studies have examined the performance of spur dikes (also known as groynes) and abutments. It seems, though, that most such studies have focused on the local flow field immediately around a dike or abutment, and on bed scour produced by such structures (e.g., Schmidt et al. 1993; Melville and Coleman 2000). Some studies have included the upstream separation region insofar that it directly affects the flow field locally at a dike or abutment. Additionally, some studies have examined how a dike, or series of dikes, might affect thalweg alignment; those studies typically have been conducted to determine dike effects on alluvial-channel bathymetry, rather than dike effects on flow field in the channel.

Considerable laboratory investigation has been devoted to scour of channels at dikes and abutments. Those investigations, however, include scant few sets of data about flow visualization and measurement at a dike or abutment over a range of scales. Relevant studies include, for example, Rajaratnam and Nwachukwu (1983); Kwan (1984); and Kwan and Melville (1994).

In recent years considerable effort has been devoted to numerical simulation of flow around a dike or abutment. Pertinent studies include those by Tingsanchali and Maheswaran (1990); Michiue and Hinokidani (1992); Muneta and Shimizu (1994); Mayerle et al. (1995); Jia and Wang (1993); Chen and Ikeda (1997); Ouillon and Dartus (1997); and Kimura and Hosoda (1999). The studies present insights into the time-averaged values of velocity immediately at a dike or abutment. They show the main features of the local flow field, but do not reveal much about dike effects on thalweg alignment or the downstream separation region. Neither do they capture the highly unsteady nature of the large-scale turbulence shed from a dike. Moreover, the numerical models presently in use do not have the capacity to simulate reliably the turbulence generated by flow around a dike, then dispersed and dissipated in the flow downstream of a dike.

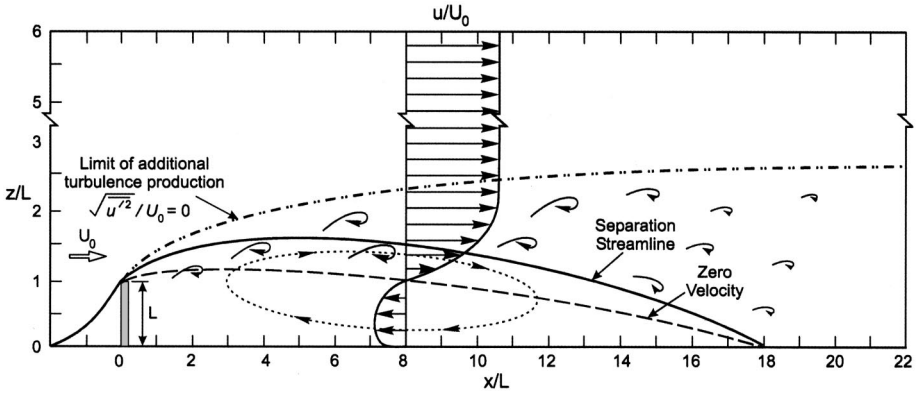

Fig. 3. Flow features produced by a low wall of length L in a uniform two-dimensional approach flow (adapted from Arie and Rouse 1956); u' is velocity fluctuation

Flow around a Barrier Wall

Studies on flow fields involving shear layers and separation regions are common for an extensive range of wall-like structures extending into flow. Information from such flow fields, especially for flow around a two-dimensional barrier wall (and axisymmetric walls such as an orifice plate in a pipe), is of potential use in explaining scale effects incurred with models of flows around dikes. Though quite a few studies describe flow features in the near field of a dike or an abutment, few studies have investigated the flow features in the broader vicinity of a dike.

Arie and Rouse (1956) describe the flow field produced by a low wall transversely placed in a uniform, two-dimensional flow in a wind tunnel test section. Low walls, like that studied by Arie and Rouse, commonly are used to modify flow, notably to hasten the development of a fully turbulent boundary layer. Arie and Rouse studied air flow in a 0.914 m wide test section for which the low wall occupied only a small portion (5%) of the local flow cross section. Fig. 3 depicts the flow field they observed around the wall, and delineates important, elemental features of flow around a linear structure like a dike.

The following features are significant for the present study:

1. The wall contracts the flow and develops two flow-separation regions, one upstream of the wall, and one downstream of it;
2. The downstream separation region produced by the wall extends about 18 lengths of the wall. This value of separation length is representative for separation regions formed by a vertical wall;
3. The wall produces turbulence, which first grows, then disperses and decays; and
4. Turbulence produced by the wall may disperse across much of the channel, including across the streamline of maximum velocity.

The velocity distribution of an approach flow can have an important influence on the flow field developed around a structure such as a wall or a dike. In this regard, it is useful to consider the body of information that exists for flow through an orifice plate in a pipe. It is well known that the discharge characteristics of orifice plates in pipes vary with those in accordance with the following parameters:

$$C_q = f\left(\frac{UD}{\nu}, \frac{k}{D}, \frac{d}{D}\right) \tag{1}$$

in which C_q = discharge coefficient for flow through the orifice; U = average velocity of approach flow; D = pipe diameter; d = orifice diameter; k = roughness height; and ν = kinematic viscosity of fluid. The first two parameters are pipe Reynolds number and relative roughness. They characterize the velocity distribution of the approach flow to the orifice; i.e., the relative magnitudes of maximum velocity and mean velocity. The third parameter is the relative opening of the orifice. Fig. 4 (Rouse 1938) shows that C_q increases as pipe diameter decreases while d/D is maintained. The increase in Cq with decreasing pipe diameter is attributable to the influence of relative roughness on approach velocity distribution. For larger k/D, the ratio of maximum velocity to mean velocity increases. Then, for constant d/D, the orifice causes less flow contraction.

The three-dimensional flow field around a dike in a flatbed open-channel flow is complicated, beyond the essentially two-dimensional flow field shown in Fig. 3, and beyond the flow field associated with orifice plates in pipes. The presence and interactions of three boundary layers (one associated with the channel bed, and two associated with the channel's walls) can influence the flow field around a dike. A further complication is the flow's free surface, whose position can adjust in response to the extent of flow constriction by a dike. These complexities may lead to scale effects for models of flow around a dike in a flatbed channel.

Similitude

The present flume experiments are based on similitude considerations used for evaluating the technical utility of small loose-bed

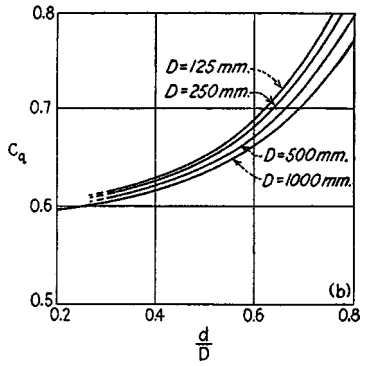

Fig. 4. Variation of pipe orifice discharge coefficient with d/D; D = pipe diameter, d = orifice diameter

models to simulate flow and sediment movement in alluvial channels. Besides the well-known concerns for Reynolds-number and Weber-number effects in small models, similitude considerations give rise to other concerns, two of which are especially important in loose-bed modeling of flow around a dike. The considerations are similitude of Froude number and of the state of bed-particle mobility; the latter criteria commonly is expressed in terms of the Shields parameter (e.g., Hydraulic Modeling 2000).

Important Variables

Most loose-bed hydraulic models focus on a few crucial processes, and attempt to simulate the important engineering variables associated with them. Hydraulic models rarely are used to simulate the full details of flow and sediment transport. In the case of micromodels (e.g., Davinroy et al. 1998), most have been used to simulate thalweg behavior along a channel whose overall width was more-or-less fixed and whose thalweg was constrained to a given alignment. Their use principally has entailed estimating the extent and number of flow-training structures, especially spur dikes, needed to constrain channel thalweg to a required depth and alignment.

For a short subreach containing one dike (Fig. 1), the following variables have major engineering significance regarding flow shift around a dike:

1. The upstream distance at which thalweg shifts from channel centerline, T_U;
2. The downstream distance required for the thalweg to realign with the channel centerline, T_D;
3. Maximum lateral location of thalweg in the short subreach, T_C; and
4. The maximum downstream extent, and lateral width, of the flow-separation region, B_1 and B_2, respectively.

For the present flatbed experiments, the thalweg is taken to be the streamline of maximum velocity around a dike in a straight rectangular channel. It is assumed that the streamline of maximum velocity, and thereby bed shear stress, would coincide with the line of deepest flow (thalweg) in an alluvial channel. The three lengths, T_D, T_U, and T_C, can be used to define the deflection of the thalweg around a single dike.

Dependencies

The important engineering variables defining thalweg depth, alignment, and sinuosity, as well as the variables defining the separation region (T_D, T_U, T_C, B_1, B_2), are dependent variables, whose values rely on so-called independent variables that characterize flow, sediment, and channel-geometry conditions prescribed by nature and/or engineers. As described below, the independent variables can be cast in general, nondimensional parameters that, taken as a whole, define sets of similitude criteria for hydraulic modeling.

The dependent variables are usefully expressed as dimensionless parameters:

$$\frac{T_D}{L}, \frac{T_C}{W}, \frac{T_U}{L}, \frac{B_1}{L}, \frac{B_2}{W}$$

An important dependent parameter of use in describing flow thalweg in a channel is the velocity ratio $U_{\max}/U$, in which $U_{\max}$ is the maximum velocity of flow along the thalweg. This parameter, with other parameters described below, expresses the distribution of approach flow to the dike.

Independent Parameters

Some loose-bed modeling, including micromodeling, customarily entails adjusting channel slope and water flow to attain a chosen level of sediment transport intensity in the model. In effect, the key flow variables adjusted are a reach-average channel slope, S_0, and a reach-average value of shear velocity, u_{*0}, for flow prior to placement of a thin dike of length L. Therefore the variables influencing flow and bathymetry in a hydraulic model of a thin dike channel, such as shown in Fig. 1, can be stated as

$$\rho, \sigma, \mu, S_0, u_{*0}, g, d, u_{*C}, W, L$$

where ρ, σ, and μ = fluid density, surface tension, and dynamic viscosity, respectively; g = gravitational acceleration; d = representative particle diameter; u_{*C} = critical value of shear velocity associated with entrainment of bed sediment; and W = channel width.

The variables lead to the following set of independent parameters results when u_{*0}, d, and ρ are used as the repeating variables in a dimensional analysis:

$$S_0, \frac{(u_{*0})^2}{gd}, \frac{u_{*0}}{u_{*C}}, \frac{\rho u_{*0} d}{\mu}, \frac{\rho d u_{*0}^2}{\sigma}, \frac{W}{d}, \frac{L}{W} \qquad \text{(Set 1)}$$

This parameter set is not entirely useful for interpreting scale effects on the flow field around a dike. Adjustment of the first two parameters brings out Froude number $\mathsf{F} = U_0/\sqrt{gR}$; here, U_0 = mean flow velocity in the channel prior to placement of the dike, and R = hydraulic radius. The combination of $S_0 = (u_{*0})^2/gR$ and $(u_{*0})^2/gd$ gives $(u_{*0})^2/gR$ and R/d. When the substitution $u_{*0} = U_0\sqrt{f/8}$ is made in $(u_{*0})^2/gR$, Froude number emerges; $U_0\sqrt{f}/\sqrt{gR} = \mathsf{F}\sqrt{f}$. In the foregoing relationships, f = a representative value of the Darcy–Weisbach resistance coefficient for flow along the channel. The parameter $W/R[= W(W+2Y)/(WY)]$ essentially expresses the aspect ratio, W/Y, of flow cross section and can be replaced by W/Y.

Parameter Set 1 therefore can be restated as

$$\frac{u_{*0}}{u_{*C}}, \mathsf{R}\sqrt{f}, \mathsf{W}f, \mathsf{F}\sqrt{f}, \frac{W}{Y}, \frac{R}{d}, \frac{L}{W} \qquad \text{(Set 2)}$$

in which $\mathsf{R} = 4U_0R/\nu$ is the Reynolds number based on flow hydraulic radius, R; and $\mathsf{W} = \rho U_0^2 L/\sigma$ is the Weber number. From Set 2, the Reynolds number readily can be written in terms of dike length. Note that f modifies the mean velocity U_0, and thereby reflects the flow resistance characteristic of the entire channel cross section; moreover, as mentioned subsequently, it plays a role in eddy formation and dissipation. R together with R/d and f characterize the approach flow distribution in which the dike is to be placed; these parameters lead to an important thalweg parameter, $U_{\max}/U_0$.

Consideration of Set 1 or 2 raises the practical issue of how indeed to attain similitude of the parameters. Similitude of an overall shear stress exerted on the flow bed (i.e., u_{*0}/u_{*C} similitude) may occur at the cost of similitude of flow field around a dike, with the upshot that pressures and velocities locally near flow boundaries are not accurately simulated. Typically, similitude based on u_{*0}/u_{*C} exaggerates U_0, and thereby amplifies stagnation-pressure heads, $(U_0)^2/2g$, generated when flow impinges against a dike or a riverbank. That amplification is partly offset by the inclusion of an energy dissipation term, $\sqrt{f}$, which too is amplified by virtue of the use of an exaggerated value of R/d.

For models requiring simulation of pressure gradients, the parameters in Set (2) can be adjusted to better express similitude of

pressure gradients. The three parameters $\mathrm{F}\sqrt{f}$, W/Y, L/W can be restated as $U_0^2 f/gL$, W/Y, L/W. These parameters are particularly useful for describing the stagnation-pressure gradient at a dike, flow aspect ratio, and dike width relative to channel width. Together with Reynolds number and Weber number they are useful for describing the modeled flow field around a dike. Additionally, flow aspect ratio, W/Y, exerts an important influence on the local flow field around a dike.

For the present study, the downstream extent of the downstream separation region, B_1, can be described functionally as

$$\frac{B_1}{L} = \mathbf{f_1}\left(\frac{u_{*0}}{u_{*C}}, \mathrm{W}f, \mathrm{F}\sqrt{f}, \mathrm{R}\sqrt{f}, \frac{W}{Y}, \frac{L}{W}, \frac{R}{d}\right) \tag{2}$$

A similar relationship can be written for the normalized, downstream distance required for the thalweg to realign with the channel centerline, T_D/L. Besides the first parameter, which expresses state of bed mobility, this equation contains essentially the same parameters expressed in Eq. (1), but adds other parameters associated with the typically nonsymmetrical cross section of a channel and the presence of a free surface. The additional parameters admit opportunities for further scale-effect trends beyond those indicated in Fig. 4 for orifice plates.

The similitude criterion $u_{*C}/u_{*0} \approx$ constant is followed tacitly for the micromodels used by the USACE and commonly by other modelers (e.g., Hydraulic Modeling 2000). The customary micromodeling procedure entails adjusting model slope and discharge until the model sediment attains an intensity of movement judged by the modeler to adequately represent bed sediment movement at full scale. As practically the same model sediment (or range of sediments) is used for simulating alluvial beds in micromodels, the relationship expressed in Eq. (2) reduces to $u_{*0} \approx \mathrm{const}_2$, because $u_{*C} \approx$ constant for the model sediment.

An observation from micromodeling practice is that average flow depths are approximately prescribed, in terms of a required flow depth associated with tow-barge navigation, or commonly occur in about the 10–30 mm range. The minimum horizontal width of the main channel in a micromodel is about 25–75 mm. Hydraulic radii nominally range from about 5 to 20 mm. The slopes of the table base holding micromodels typically are in the range of about 0.01, and $u_{*0} \approx 2.0 \times 10^{-2}$ to about 5×10^{-2} m/s. These dimension ranges, together with Eq. (2), were used in designing the program of flume experiments for the present study.

Flume Experiments

The preceding considerations of dimensional analysis, similitude criteria, and scale effects indicate the difficulties potentially faced in using hydraulic models to simulate flow around a dike in an alluvial channel. Because modeling, especially with small models, is primarily based on about one or two similitude criteria, scale-effects arise. To date, there appears to be no study that documents scale-effect trends for the flow features shown in Fig. 1.

The present experiments were conducted to delineate such trends, and are based primarily on the similitude criterion $u_{*0}/u_{*C} \approx$ const. They sought to chart deviations in simulation accuracy of the parameters T_D/L, T_U/L, T_C/W, B_1/L, and B_2/W for a single dike in a flatbed channel. The experiments are a necessary precursor to experiments with a dike in a loose-bed channel, as the scale-effect trends associated with the flow-field parameters $U_0^2 f/gL$, W/Y, and L/W should first be determined for the baseline case uncomplicated by changes in bed morphology. Those changes, notably bed scour in the vicinity of the dike and bed form movement, would obscure the influences of the flow-field parameters.

The experiments were conducted using two flumes fitted to contain a rectangular, straight channel containing a spur dike aligned at 90° to one side of the channel, as illustrated in Fig. 1. The dike extended across one-third of the channel width. This condition of a relatively long dike is fairly common for dikes used for channel control along the Mississippi and Missouri Rivers (USACE, personal communication). The bulk of the experiments were conducted using a flume whose dimensions enabled replication of flow for an adequately large range of length dimensions, and thereby length scales. The setup and conduct of the flow cases associated with the smallest dimensions of channel and dike were done using a small flume that enabled better control of flow conditions associated at such small dimensions.

The principal flatbed flume is 30.0 m long, 0.91 m wide, and 0.45 m deep. The flume has glass-sided walls and a smooth aluminum bed. The smaller flume was formed in a 1.6 m long by 0.98 m wide by 0.15 m deep water table; inserts formed a flume narrowed to 30 mm.

Before the dike was inserted in the flow established in each flume, the channel-average shear velocity for the flow associated with each experiment was calculated as $u_{*0} = \sqrt{gRS_0}$, in which $R =$ hydraulic radius of flow. For each combination of horizontal and vertical length scales X_r and Y_r, the channel within the flume was set to a prescribed width. Then, flow discharge and flume slope were set to produce the required uniform depth of flow along the channel. Flow uniformity was verified by comparing the free-surface slope and the flume's bed slope. Flow depths were measured at centerline points along the flume. Flume slope and flow rate were adjusted in an iterative manner until the requisite uniform flow was attained. A consequence of this procedure was increased value of bulk average velocity of flow and a corresponding increase in flow Froude number. The bulk velocity of flow was calculated using Manning's equation, $U_0 = R^{2/3} S_0^{1/2}/n$. The value of the Manning's coefficient, n, for each experimental channel was calculated from the flow conditions to be 0.012, commensurate with the smooth metal finish of the flume and the water table.

The Reynolds numbers associated with flow in the channel was calculated as

$$\mathrm{R} = \frac{4U_0 R}{\nu} = \frac{4U_0 A}{\nu P} = \frac{4Q}{\nu P} \tag{3}$$

For flow around the model dike, the Reynolds number is taken as

$$\mathrm{R}_{\mathrm{dike}} = \frac{U_0 L}{\nu} \tag{4}$$

The results are keyed to a baseline flow field (Fig. 5), herein taken to be representative of the flow field around a full-scale dike in a fixed, flat-bottomed channel of rectangular cross section. The baseline flow field corresponded to the following hydraulic conditions: $W = 0.91$ m, $Y_0 = 0.15$ m, $\overline{u}_{*0} = 0.01$ m/s, $\mathrm{F} = 0.20$, $\mathrm{R} = 1.5 \times 10^5$, $R_{\mathrm{dike}} = 0.75 \times 10^5$, $W/Y_0 = 6$, and $W/L = 3$. For these conditions, horizontal and vertical length scales are herein designated, respectively, as $X_r = 1$ and $Y_r = 1$. Relative to these baseline values, the experiments were conducted over a range of five horizontal scales and four vertical scales; i.e., $X_r = 1$, 4, 8, 12, and 24 and $Y_r = 1$, 2, 3, and 6.

The thalweg alignment and the areal extent of the separation region downstream of the simulated dike were observed and recorded by way of video-tracking of drogues (1-mm-diameter

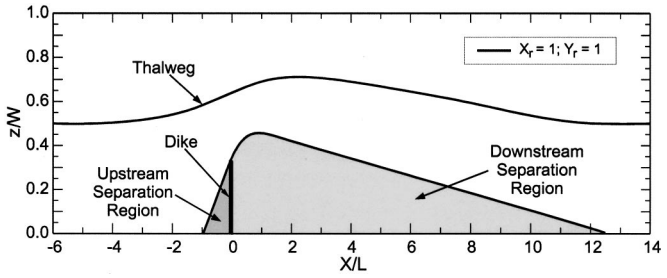

Fig. 5. Thalweg alignment and separation zones for flatbed baseline condition

polyethylene beads) released in the flow, and large-scale particle image velocimetry (LSPIV). Figs. 6(a and b) show both a normal perspective of 0.9-m-wide flume with lighting arrangement for the tracking and an image transformation used for LSPIV estimation of the pair of flow features. Each pair of flow features was observed and recorded for 10–12 min, and average values then determined for thalweg alignment and the extent of the downstream separation region.

Results

Presented first are the flow distributions and the values of the aforementioned parameters for the baseline flow field. Considered

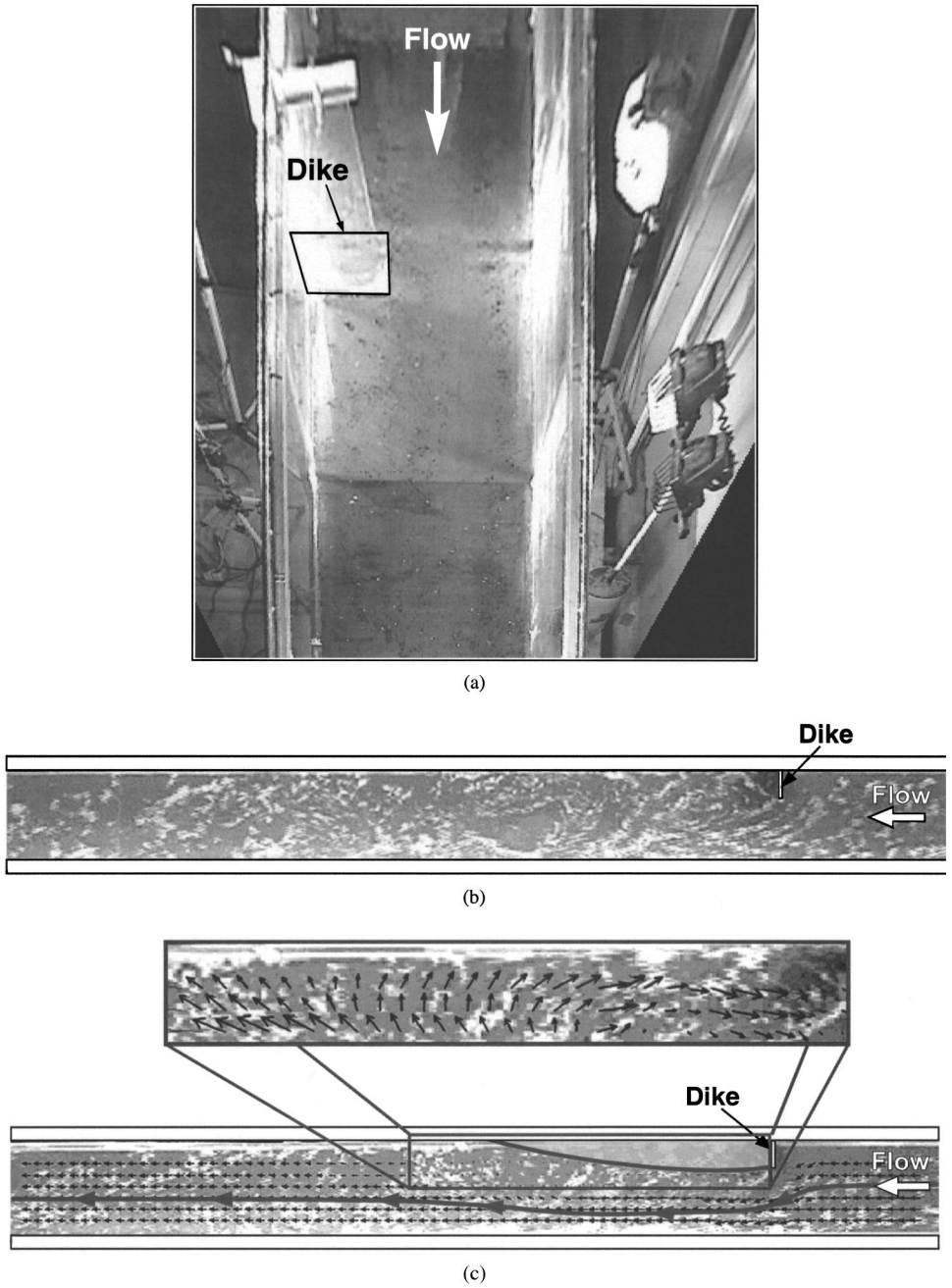

Fig. 6. View of two flows set at $u_* = 0.01$ m/s: (a) 0.9 m flume and a model dike and after image transformation for large-scale particle image velocimetry (LSPIV) analysis of black tracer drogues; (b), view of 0.030-m-wide flume with white tracers (for LSPIV) showing dike eddies dispersing across full width of channel; and (c) velocity vectors obtained from tracers using LSPIV.

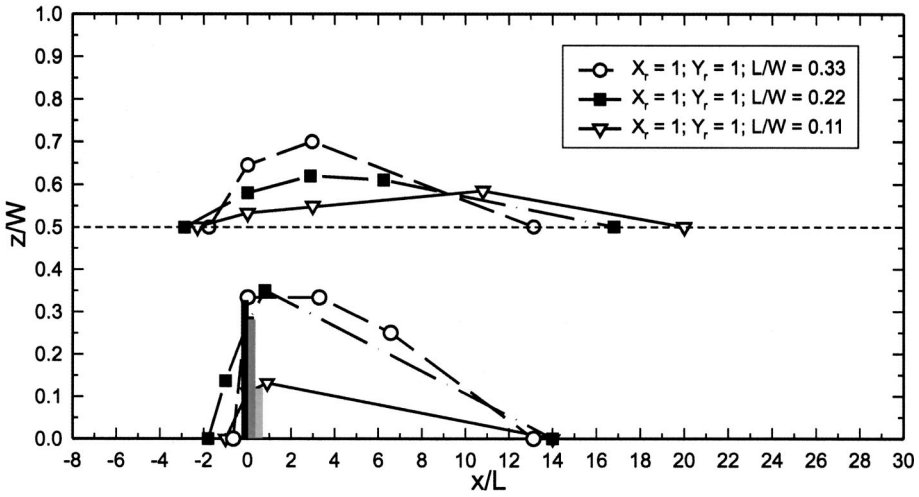

Fig. 7. Variation of thalweg alignment and flow-separation regions with L/W

subsequently are baseline-parameter sensitivities to dike length and variations of F and $\overline{u}_{*0}/u_{*C}$ (in effect $\overline{u}_{*0}$, as u_{*C} is constant). The sensitivities are considered for ranges of values occurring in the ensuing scale-effect experiments, and were examined to ensure that the selected baseline condition of flow is suitably general and, for the purpose of the study, itself free of significant scale effects. The bulk of the results concern the sensitivities of T_D/L, T_C/W, T_U/L, B_1/L, and B_2/W to reductions in X_r and Y_r, with flow for each case set at $\overline{u}_{*0}=0.01$ m/s. The results are presented in sets associated with four flow depths or vertical scales, Y_r. For this series of experiments, flume width, length dike, depth, and a bulk value of shear velocity were prescribed. Flow discharge and flume slope were adjusted until uniform flow occurred for the prescribed. Then the model dike was placed in the flume.

Baseline Flow

As expected, the dike laterally displaced the flow, locally contracted it, and thereby deflected the thalweg to approximately, as indicated in Fig. 5, $T_C/W\approx 0.74$. The maximum lateral extent of the flow-separation region is about $B_2/W\approx 0.34$, or $B_2/L=1.1$. In due course, the thalweg re-aligned downstream with the channel centerline at a channel location coinciding with the downstream extent of the flow-separation region, $B_1/L\approx 13$. These values of B_1/L and B_2/W concur fairly well with the values often cited for extent of flow separation region; e.g., Arie and Rouse (1956) indicate $B_1/L=18$, $B_2/L=1.6$; and, from numerical simulation Chen and Ikeda (1997) indicate $B_1/L=14$. The proximity of the far wall likely would reduce B_1/L and B_2/L for the baseline condition, compared to the flow measured by Rouse. Further details of the flow field are reported by Ettema and Muste (2002).

Sensitivity Tests

The baseline flow field was checked to determine whether the overall structure might be sensitive to limited variations of dike length, L and, for a given dike length, to variation of Froude number, F, and $\overline{u}_{*0}$. Three values of L/W were examined, $L/W=0.33$, 0.22, and 0.11. The results presented in Fig. 7 show that increasing L/W increases the lateral displacement of thalweg alignment, B_2/W, but does not significantly alter T_D/L, which remains at about 13 to 14. Conversely, however, relative to dike length, the upstream influence of the dike slightly decreases with increasing L/W; i.e., T_U/L decreases, though the results are not entirely clear due to the dike's protrusion into varying lateral distributions of approach velocity. This latter trend can be explained in terms of the magnitude of stagnation pressure head developed at the dike. The average value of the stagnation head at the dikes was slightly larger for the longer dike, as area average velocity of approach flow increased with distance out from the flume wall.

All other parameters held constant for the range of values considered here, Froude number exerted no pronounced effect on thalweg alignment and the extent of the downstream flow-separation region. Fig. 8 shows the thalweg alignment and the extent of downstream flow-separation region for the ranges $\overline{u}_{*0}=0.01$, 0.02, and 0.3m/s, and F=0.20, 0.40, and 0.60. The dike's influence on flow thalweg alignment extends about the extent of the flow-separation region downstream of the dike. The downstream extent of the flow separation region, $B_1/L\approx 13$ to 14, is slightly shorter than the flow separation region shown in Fig. 4 for the two-dimensional flow of air over a low wall (Arie and Rouse 1956). The maximum deflection of the thalweg line, T_C/W, is to about 0.7.

The results shown in Figs 7 and 8 confirm that the flow condition selected as the baseline condition for the experiments is adequately consistent and comparatively insensitive to flow variations for the ranges of W/L and F considered. Consequently, it was decided to proceed with the baseline flow condition as the benchmark flow for investigating how thalweg alignment and extent of flow separation region (variables) may vary with reductions in horizontal length scale, X_r, and vertical length scale, Y_r, in small models whose primary criterion for dynamic similitude is $u_{*0}/u_{*C}\approx$ const. In lieu of flow-field data from an actual dike, the baseline condition is taken herein to be the prototype flow condition.

Length-Scale Data

The length-scale data indicate an increasing difficulty in simulating thalweg alignment and extent of separation region with increasing length scales, X_r and Y_r, owing to the increased large-scale turbulence with scale increase. The data are presented in Figs. 9–12, which show thalweg alignments and extents of sepa-

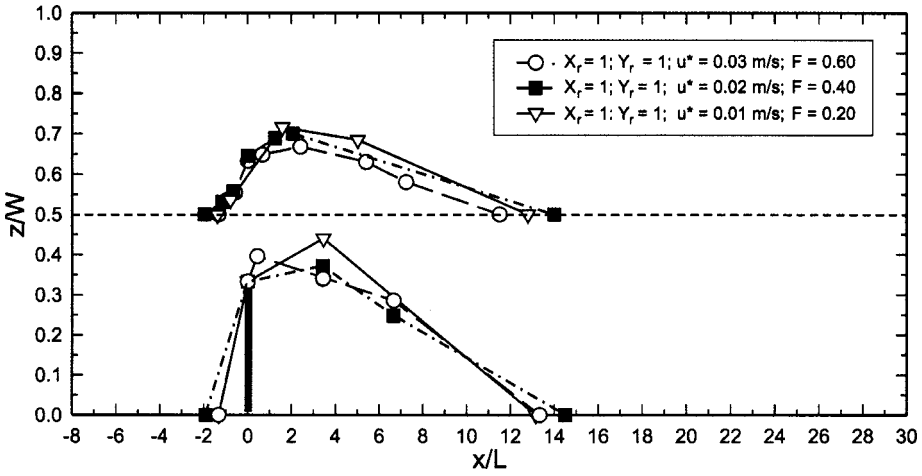

Fig. 8. Thalweg and separation-region variation with Froude number F

ration regions recorded for variable length scales X_r and Y_r, but with the same bulk value of $u_*=gRS=0.01$ m/s. For each figure, X_r is varied by narrowing the channel and shortening the dike (W/L held at 0.33), while flow depth (vertical scale Y_r) is constant. The figures show the streamwise trajectory of the thalweg line normalized with flume width (top plot in figures), and the extent of the separation areas normalized with length of the dike (bottom plot in figures).

For the range of length scales and channel dimensions considered in the present study, the data indicate consistent scale-effect trends, showing that horizontal-length scale X_r and vertical scale Y_r affect flow thalweg alignment and separation regions around a hydraulic model of a dike in a flatbed channel. The trends are of use in interpreting the results from hydraulic models.

Thalweg Alignment

Model scales less than the baseline scales caused the thalweg alignment to deviate from the benchmark alignment. The trends are presented in Figs. 13(a and b), which for purposes of scale alsoindicates a $\pm 10\%$ margin of error. That error margin is chosen in direct relationship with the accuracy of the instrumentation used in the experiments.

The parameter T_D/L relative to the parameter's benchmark value, $(T_D/L)_b$, increases with increasing X_r. The ratio, $[(T_D/L)]/[(T_D/L)_b]$, also increases with Y_r over the range of flow dimensions considered in this study. It attains a maximum value of almost 3 when $X_r=24$ and $Y_r=6$. In other words, the flow around a very small hydraulic model dike (such as in micromodels) in a flatbed channel does not replicate the thalweg alignment around the dike. The thalweg requires almost three times the benchmark value of T_D/L in order to return to the channel centerline downstream of the dike.

With regard to lateral extent of thalweg, the parameter T_C/L relative to the parameter's benchmark value, $(T_C/L)_b$, is comparatively insensitive to horizontal and vertical scales X_r and Y_r. At the maximum value of horizontal scale $X_r=24$, the ratio is about 1.2. If anything, the value of ratio $[(T_C/L)]/[(T_C/L)_b]$

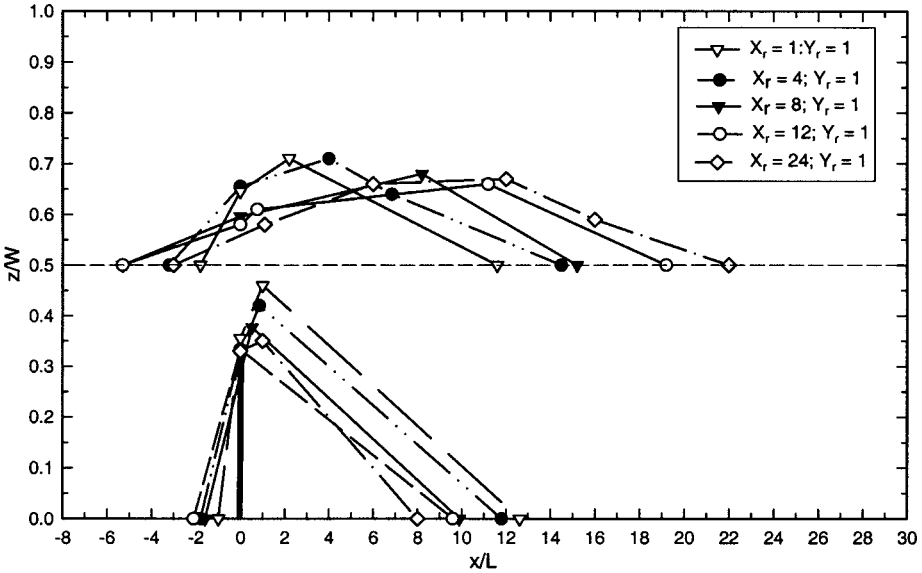

Fig. 9. Thalweg alignment and separation regions, $Y_r=1$ ($Y_0=0.15$ m)

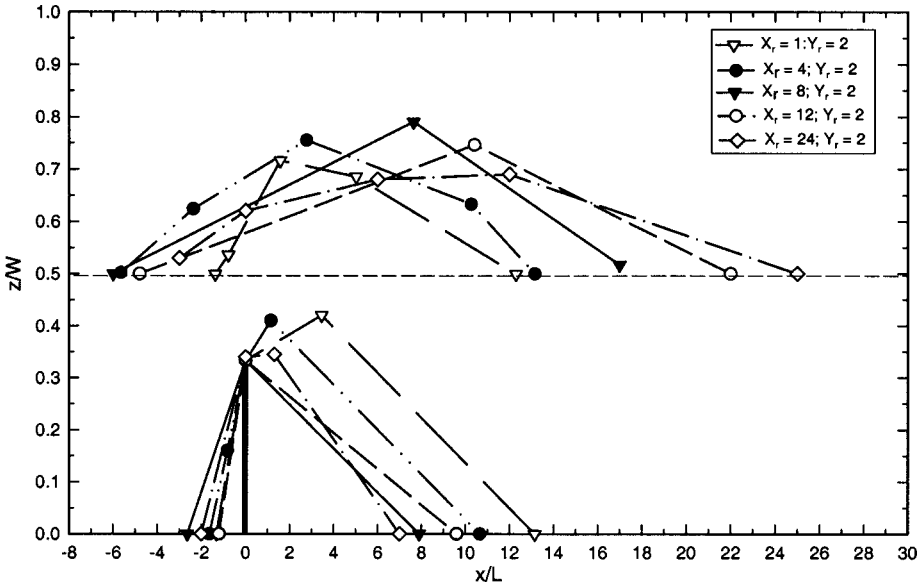

Fig. 10. Thalweg alignment and separation regions, $Y_r=2$ ($Y_0=0.075$ m)

mildly reduces as X_r increases up to about 12, before increasing. The comparative insensitivity, and decrease, of T_C/L with respect to X_r is to be expected for two reasons. The flow is constrained by the rigid dike, which extends across a third of the channel, and rigid flume wall, and therefore does not have much latitude to adjust.

Fig. 13(a) shows that when $Y_r=1$, the thalweg alignment parameter T_D/L departs from its baseline values when X_r exceeds about 8. The baseline value allows for an error margin of $\pm 10\%$. The figure also shows that modeling error occurs for lesser values of X_r and Y_r increases.

Downstream Separation Region

Figs. 14(a and b) show that the downstream length of the separation region, B_1/L, shrinks continuously in streamwise length as horizontal scale, X_r, increases. Additionally, it decreases as vertical scale, Y_r, decreases, as shown in Fig. 13(b) only for the set of tests $X_r=1$. The other cases were not plotted because the differences in the maximum lateral extent were minor, and within the uncertainty of the instrumentation and experimental methods employed.

The maximum lateral extent of the separation region, B_2/W, decreases with increasing X_r and Y_r, until $B_2/W \approx L/W$; i.e., the separation region does not extend out beyond the dike. The separation-region parameter B_1/L is quite sensitive to length scales, and distorts beyond the 10% margin when X_r exceeds about 4 and $Y_r=1$. Moreover, the distortion occurs earlier as Y_r increases.

Scale-Effect Trends

The trends obtained for thalweg alignment and extent of separation region [Figs. 13(a and b) and 14(a and b), respectively] are explainable in terms of the turbulence formed in, and dispersed

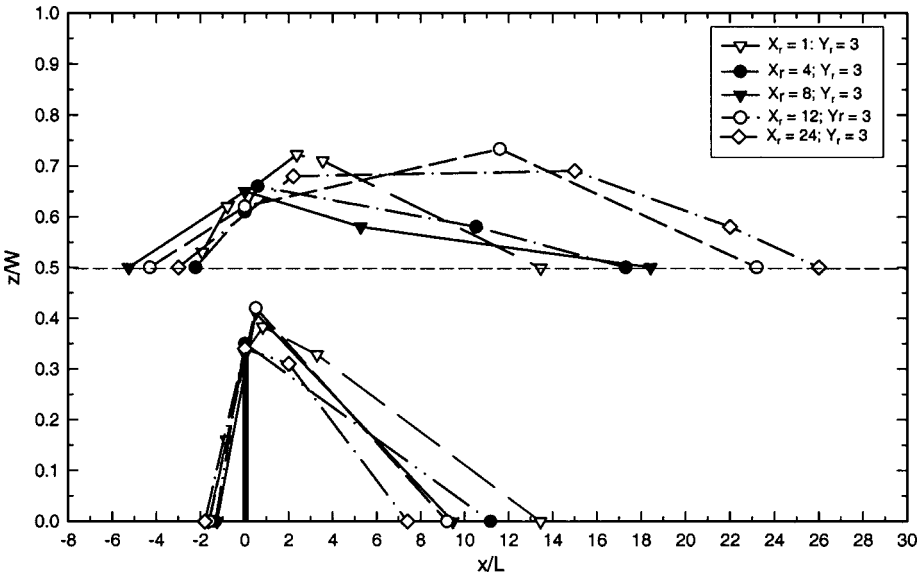

Fig. 11. Thalweg alignment and separation regions, $Y_r=3$ ($Y_0=0.05$ m)

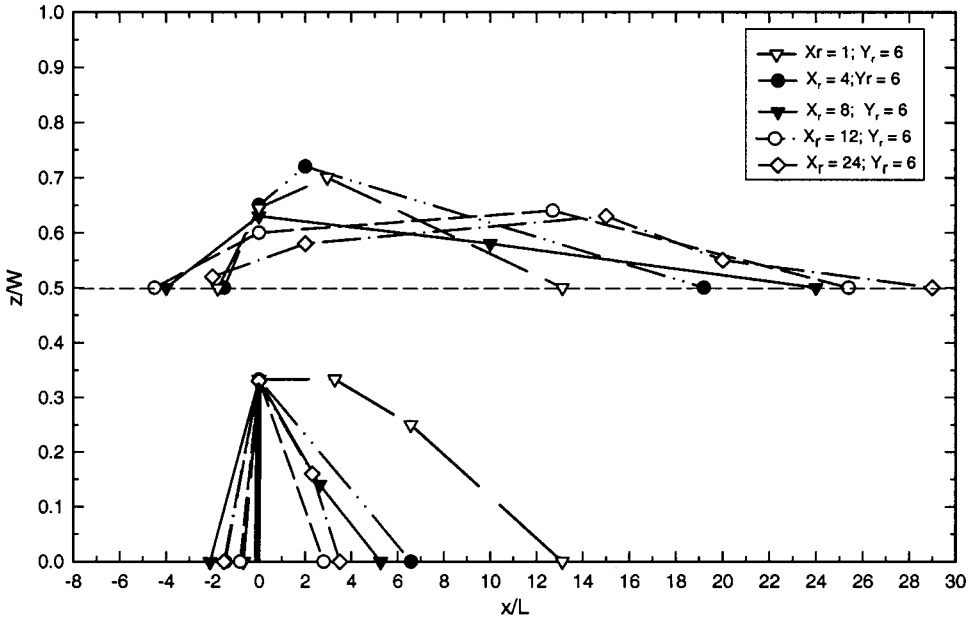

Fig. 12. Thalweg alignment and separation regions, $Y_r = 6$ ($Y_0 = 0.025$ m)

from, the wake eddy formed by the model dike. That turbulence influences the length of flow needed for the thalweg to return to the center channel and flow symmetry to be reestablished downstream of the dike.

The complexity of the flow field is indicated in Fig. 15, a schematic sketch of turbulence generated by the model dike. The flatbed flow field approaching the dike comprises three boundary layers, one formed from the bed and each of the two walls. Furthermore, dike presence affects the approach-flow field. As a dike constricts flow it creates a backwater effect, which increases with increasing dike length. This effect influences the pressure distribution around a dike, and thereby influences the local flow immediately at a dike; i.e., the formation of separation eddies, rollers, various submerged vortices, and vertical components of flow at the dike. Yet to be investigated in this regard are the effects associated with the presence of the resistance coefficient f included in several of the parameters in Eq. (2). One effect concerns the

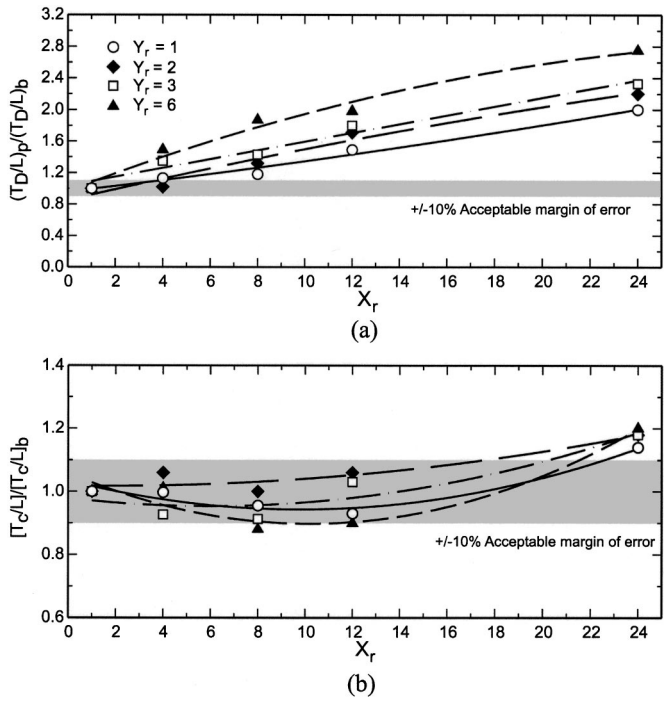

Fig. 13. Effect of length scales on thalweg alignment: (a) normalized length of thalweg disturbance downstream of dike and (b) normalized distance of thalweg line across channel

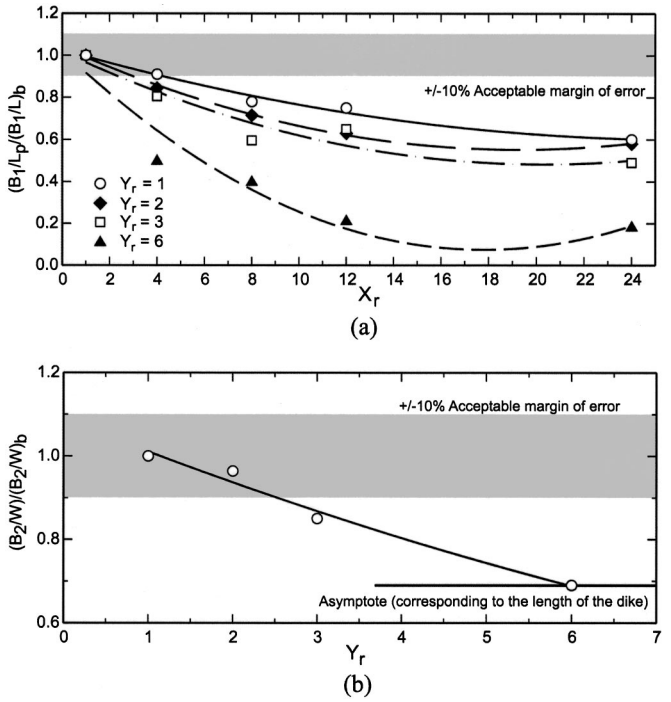

Fig. 14. Effects of length scales on extent of downstream separation region: (a) normalized length of separation region downstream of dike and (b) normalized width of separation region across channel

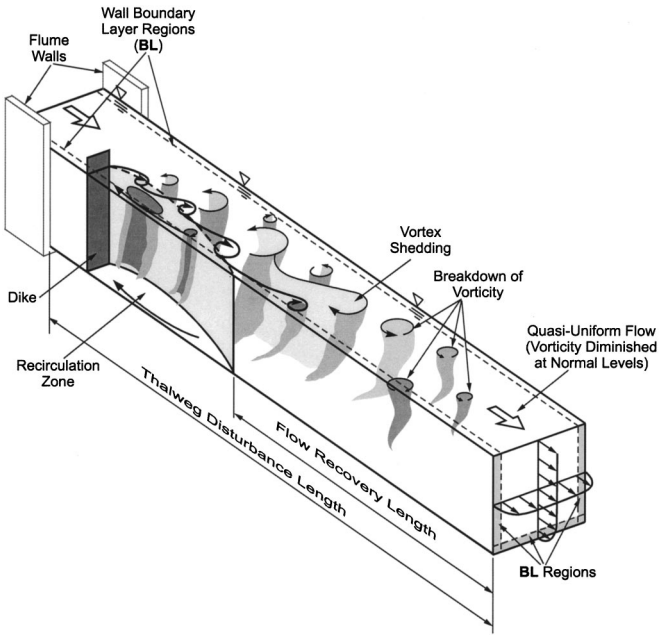

Fig. 15. Three-dimensional nature of approach flow complicates similitude for modeling flow around a single dike in a flatbed channel

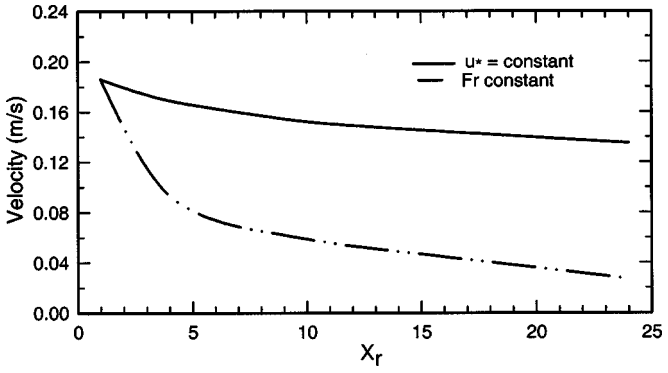

Fig. 16. Comparison of the bulk velocity of flow in the model, for similitude based primarily on u_*/u_{*C} constant or Froude number constant.

formation and dissipation of turbulence generated by a dike. The literature on similitude of flow around dike-like structures does not address this effect.

Explanation of the trends in Figs. 13(a and b) and 14(a and b) requires consideration of the conflicting requirements of similitude criteria evident in Eq. (2), by way of example for one aspect of thalweg alignment. In particular, values of both u_{*0}/u_{*C} and F cannot be maintained when modeling from field to flume. The criteria conflict is troublesome for modeling of one-dimensional (up/down) changes in bed elevation flow, but can be taken into account by way of model calibration. However, the conflict becomes especially severe in modeling local, two-or three-dimensional behavior of flow and bed behavior at larger values of X_r and possibly Y_r.

These considerations can complicate interpretation of scale-effect trends, even for flows in which Reynolds number and Weber number effects arguably are not significant. Variations in approach-flow condition, boundary (bed, wall, and dike) roughness, and dike geometry may influence the specific values of thalweg alignment and flow-separation extents for a given baseline case. However, those values should undergo the same trends as model length scales X_r and Y_r alter.

For loose-bed models it is imperative to simulate intensity of bed sediment movement, there is little alternative than to base dynamic similitude on u_{*0}/u_{*C} rather than on $U_0^2 f/gL$. The inevitable consequence of so doing is larger values of U_0 in a model than required by the Froude-number criterion. Fig. 16 shows that the actual values of bulk velocity, U_0, used in the models exceed the values of U_0 specified from Froude number similitude criterion for the range of X_r used in the flume experiments. The disparity, or exaggeration of U_0, is larger for increased X_r. It is important to mention that, in absolute value, U_0 actually decreases as X_r increases, but that U_0 exceeds the value prescribed in accordance with Froude-number similitude.

An exaggeration of U_0, with increasing X_r, leads to amplification of velocity heads of flow. Velocity heads are proportional to U_0^2, and they set the magnitudes and gradients of pressure around a structure in the flow. Pressure magnitudes and gradients determine the magnitudes of local-flow velocities and intensities of turbulence.

The decrease in aspect ratio W/L with increasing X_r and constant Y_r further increases the velocity head (or headloss) associated with flow around the dike. In turn, this effect increases flow backwater elevation, increases the upstream extent of the upstream separation region, produces a more uniform distribution of flow velocity through the flow constriction caused by the dike, and thereby shifts the thalweg closer to the dike. In so doing, it reduces the width of the downstream separation region.

The consequences of exaggerated velocity head for thalweg alignment and extent of downstream separation region are explainable in terms of Fig. 15 and the following points:

1. Exaggerated velocity head and flow aspect ratio (as expressed in parameters $U_0^2 f/gL$ and W/Y) leads to increased vorticity of wake eddy formed by the dike. Increased vorticity of wake eddy causes the eddy to contract the downstream separation region behind the dike.
2. Increased vorticity of the wake eddy intensifies flow turbulence shed from the dike, which then is dispersed further, relative to dike length, along and across the flow downstream of the dike. The increase in the larger scale vorticity downstream of the dike is enhanced by the wall-induced vorticity, which is a parameter not directly controlled in the model, and which plays an increasing influence in the overall vorticity budget as model scale increases (model size decreases). This relative increase in turbulence dispersion entrains more slower moving water into the flow passing around the dike, which thereby delays the overall reestablishment of flow symmetry downstream of the dike, and in so doing retards thalweg return to the channel centerline. A consequence of increased turbulence intensity is the growing divergence of thalweg alignment and extent of the downstream separation region.

The flow distribution at the end of the separation region is markedly skewed, velocities locally being larger towards the wall across from the dike. Eddies and turbulence generated by the dike and a shear layer downstream of it disperse across the flow. As with boundary layer development, the mixing action of turbulence causes small water masses to be swept back and forth from a low velocity zone outward into a higher velocity zone. Through an exchange of momentum, the slow water acts as a retarding shear stress applied to the faster flow. As the eddies and turbulence

intensify, and take longer (relative to dike length) to decay, this momentum-exchange process extends over a relatively longer downstream distance, and thereby slowing the readjustment of a more-or-less uniform streamwise distribution of flow. It was observed from the experiments that, as X_r decreased, turbulence eddies were dispersed further across the model channel. For the smallest scales, eddies reached the far wall before decaying.

Conclusions

The present study was conducted to determine how length scales influence selected important features of the flow field in hydraulic models of a single spur dike placed in a flatbed channel, and when such models are operated primarily in accordance with dynamic similitude based on a level of bed shear stress (or shear velocity), rather than Froude number. The flow features of interest are thalweg alignment (the path of maximum flow depth and usually maximum velocity) of flow around a dike, and flow-separation region formed immediately downstream of a dike. These features are of major significance for alluvial-channel control. Because the study was conducted in the context of better understanding the facility of small hydraulic models to simulate flow and sediment movement around a dike in a loose-bed channel, the flume experiments conducted for the study used the same primary similitude criterion used for loose-bed hydraulic models; i.e., $u_{*0}/u_{*C} \approx \text{const}$.

The study's principal conclusions are as follows:

1. When approximate constancy of the parameter u_{*0}/u_{*C} is the primary similitude criterion used to operate a model for a dike of given W/L, distortion of the other flow parameters in Set 3 may influence thalweg alignment and separation region. The distortions, which essentially stem from natural limitations in scaling sediment size, may cause scale effects that increase in influence as length scales (prototype/model) increase.
2. The scale effects for a dike in a flatbed channel become evident as the following deviations (values in model compared to scaled prototype values) in thalweg alignment and separation regions:
   - As X_r increases, flow thalweg requires a longer distance, relative to dike length, to return to the channel centerline downstream of a dike. The distance downstream of the dike, T_D/L, was almost three times as long for the channel equivalent to a micromodel than for the baseline channel.
   - As X_r increases, the maximum lateral location of the thalweg, T_C, decreases until an asymptotic value of approximately $(W-L)/2$.
   - As X_r increases, the downstream flow-separation region contracted from $B_1/L \approx 14$ for the baseline channel to $B_1/L \approx 4$ for the channel equivalent to a micromodel.
   - As X_r increases, the width of the flow-separation region decreased asymptotically to the length of the dike (i.e., $B_2/L \rightarrow 1$).
3. The flow parameters in Set 3 directly affect the distribution of pressure and local flow structure around the upstream face of a dike. Through that action, they affect the strength of wake eddies developed by a model dike. In consequence, the dike's wake region contracts in extent. The shedding of strengthened wake eddies intensifies turbulence generated by the model dike. Increased turbulence generation and increased dispersion of turbulence results in a longer flow length, relative to dike length, for flow symmetry to reestablish downstream of a dike. Commensurately, it takes longer for flow thalweg to return to channel centerline.

Acknowledgments

The writers thank the reviewers of this paper. The review comments substantively strengthened the paper and indicated opportunities for further investigation of issues regarding hydraulic modeling of flows markedly influenced by large-scale turbulence.

References

Arie, M., and Rouse, H. (1956). "Experiments on two-dimensional flow over a normal wall," *J. Fluid Mech.* 1(2), 129–141.

Brinke, W. B., ten Kruyt, N. M., Kroon, A., and van den Berg, J. H., (1999). "Erosion of sediment between groynes in the River Waal as a result of navigation traffic." *Special Publ. 28*, Int. Association of Sedimentologists, 147–160.

Chen, F-Y., and Ikeda, S. (1997). "Horizontal separation flows in shallow open channels with spur dikes." *J. Hydrosci. Hydr. Eng.*, 15(2), 15–30.

Davinroy, R. D., Gordon, R. C., and Hetrick, R. D. (1998). "Sedimentation study of the Mississippi River, Marquette Chute: Hydraulic micromodel investigation." *Tech. Rep. M3*, Applied River Engineering Center, St. Louis District, U. S. Army Corps. of Engineers, St. Louis.

Ettema, R., and Muste, M. (2002). "Scale-effect trends on flow thalweg and flow separation at dikes in flatbed channels." *IIHR Rep. 414*, IIHR–Hydroscience and Engineering, The Univ. of Iowa, Iowa City, Iowa.

Hydraulic Modeling (2000). *Hydraulic modeling: Concepts and practice*, ASCE, Reston, Va.

Jia, Y., and Wang, S. S. (1993). "3D numerical simulation of flow near a spur dike." *Proc., 1st Int. Conf. on Hydro-Science and Engineering*, Washington, D.C., 2150–2156.

Kimura, I., and Hosoda, T. (1999). "3-D unsteady flow structures around rectangular column in open channels by means of non-linear k-ε model." *Proc. 1st Int. Symposium On Turbulence and Shear Flow Phenomena*, Santa Barbara, Calif., 1001–1006.

Kwan, T. W. (1984). "A study of abutment scour." *Rep. 451*, School of Engineering, The University of Auckland, New Zealand.

Kwan, T. W., and Melville, B. W. (1994). "Local scour and flow measurements at bridge abutments." *J. Hydraul. Res.*, 32(5), 661–673.

Mayerle, R., Toro, F. M., and Wang, S. S. (1995). "Verification of a three dimensional numerical model simulation of the flow in the vicinity of spur dikes." *J. Hydraul. Res.*, 33(2), 243–256.

Melville, B. W., and Coleman, S. (2000). *Bridge scour*, Water Resources Publications, Littleton, Colo.

Michiue, M., and Hinokidani, O. (1992). "Calculation of 2-dimensional bed evolution around spur-dike." *Annu. J. Hydraul. Eng. Jpn. Soc. Civ. Eng.*, 36, 61–66.

Muneta, N., and Shimizu, Y. (1994). "Numerical model with spur-dike considering the vertical velocity distribution." *Proc., Japan Society of Civil Engineers Conf.*, Tokyo, 497, 31–39.

Ouillon, S., and Dartus, D. (1997). "Three-dimensional computation of flow around groyne." *J. Hydraul. Eng.*, 123(11), 962–970.

Rajaratnam, N., and Nwachukwu, B. A. (1983). "Flow near groin-like structures." *J. Hydraul. Eng.*, 109(3), 463–480.

Rouse, H. (1938). *Fluid mechanics for hydraulic engineers*, McGraw–Hill, New York.

Schmidt, J. C., Rutin, D. H., and Ikeda, H. (1993). "Flume simulation of recirculating flow and sedimentation." *Water Resour. Res.*, 29(8), 2925–2939.

Tingsanchali, T., and Maheswaran, S. (1990). "2-D depth-averaged flow computation near groyne." *J. Hydraul. Eng.*, 116(1), 71–86.

Uijttewaal, W. S., Lehmann, D., and van Mazijk, A. (2001). "Exchange processes between a river and its groyne fields: Model experiments." *J. Hydraul. Eng.*, 127(11), 928–936.

Copyright of Journal of Hydraulic Engineering is the property of American Society of Civil Engineers and its content may not be copied or emailed to multiple sites or posted to a listserv without the copyright holder's express written permission. However, users may print, download, or email articles for individual use.